ISSCR

An *In Vitro* Human Liver Model by iPSC-Derived Parenchymal and Non-parenchymal Cells

Yuta Koui,[1] Taketomo Kido,[1,*] Toshimasa Ito,[1] Hiroki Oyama,[1] Shin-Wei Chen,[1] Yuki Katou,[2] Katsuhiko Shirahige,[2] and Atsushi Miyajima[1,*]

[1]Laboratory of Cell Growth and Differentiation, Institute of Molecular and Cellular Biosciences, The University of Tokyo, Tokyo 113-0032, Japan
[2]Laboratory of Genome Structure and Function, Research Center for Epigenetic Disease, Institute of Molecular and Cellular Biosciences, The University of Tokyo, Tokyo 113-0032, Japan
*Correspondence: kido@iam.u-tokyo.ac.jp (T.K.), miyajima@iam.u-tokyo.ac.jp (A.M.)
http://dx.doi.org/10.1016/j.stemcr.2017.06.010

SUMMARY

During liver development, hepatoblasts and liver non-parenchymal cells (NPCs) such as liver sinusoidal endothelial cells (LSECs) and hepatic stellate cells (HSCs) constitute the liver bud where they proliferate and differentiate. Accordingly, we reasoned that liver NPCs would support the maturation of hepatocytes derived from human induced pluripotent stem cells (hiPSCs), which usually exhibit limited functions. We found that the transforming growth factor β and Rho signaling pathways, respectively, regulated the proliferation and maturation of LSEC and HSC progenitors isolated from mouse fetal livers. Based on these results, we have established culture systems to generate LSECs and HSCs from hiPSCs. These hiPSC-derived NPCs exhibited distinctive phenotypes and promoted self-renewal of hiPSC-derived liver progenitor cells (LPCs) over the long term in the two-dimensional culture system without exogenous cytokines and hepatic maturation of hiPSC-derived LPCs. Thus, a functional human liver model can be constructed *in vitro* from the LPCs, LSECs, and HSCs derived from hiPSCs.

INTRODUCTION

As hepatocytes exhibit numerous functions, including expression of various metabolic enzymes such as a number of cytochrome P450 oxidases responsible for the biotransformation of various compounds as well as drugs, primary cultures of human hepatocytes have been used for drug discovery and toxicology. However, primary cultured hepatocytes exhibit very limited metabolic activity, and the supply of human hepatocytes is also limited. To overcome these problems, researchers have made efforts to generate functional hepatocytes from human induced pluripotent stem cells (hiPSCs) (Ogawa et al., 2013; Si-Tayeb et al., 2010; Takayama et al., 2012). We previously identified carboxypeptidase M (CPM) as a cell-surface marker for liver progenitor cells (LPCs) to induce hepatocytes from iPSCs effectively (Kido et al., 2015; Tanaka et al., 2007). As CPM+ cells derived from hiPSCs exhibit potential to proliferate and differentiate to both hepatocyte-like and cholangiocyte-like cells, hiPSC-derived CPM+ cells are considered LPCs (Kido et al., 2015). While hepatocytes derived from CPM+ LPCs exhibit much higher metabolic activity compared with those derived from hiPSCs using a conventional protocol, the levels of some mature hepatic functions are still not as high as those in primary human hepatocytes.

In mice, liver development starts with the hepatic specification of the foregut endoderm at embryonic day 8.5–9.0 of gestation (E8.5–E9.0) (Tremblay and Zaret, 2005). Hepatoblasts are embryonic LPCs derived from endoderm cells, which proliferate and migrate into the *septum transversum*

mesenchyme to form the liver bud. They become mature hepatocytes and cholangiocytes through interactions with hepatic non-parenchymal cells (NPCs) such as liver sinusoidal endothelial cells (LSECs) and hepatic stellate cells (HSCs). Previous studies showed impaired hepatic differentiation in mutant mice lacking LSECs or HSCs (Hentsch et al., 1996; Matsumoto et al., 2001), revealing important roles for NPCs in liver development. In the present study, toward generation of hiPSC-derived mature hepatocytes, we generated hiPSC-derived LSECs and HSCs capable of supporting the proliferation and differentiation of LPCs.

RESULTS

Isolation of LSEC Progenitors and HSC Progenitors from Mouse Fetal Livers

Because LSEC progenitors and HSC progenitors are present in the liver bud where they proliferate and differentiate into mature LSECs and HSCs, respectively, it would be useful if such cells could be derived from hiPSCs. To establish culture systems for LSEC progenitors and HSC progenitors, we searched for cell-surface molecules that would be useful for the identification and isolation of these progenitors. We have previously reported that LSEC progenitors express endothelial markers such as FLK1, CD31, and CD34 (Nonaka et al., 2007), and ALCAM+ *septum transversum* mesenchymal cells were shown to give rise to HSCs during fetal liver development (Asahina et al., 2011). As shown in Figure 1A, flow-cytometric (FCM) analysis showed that

CrossMark
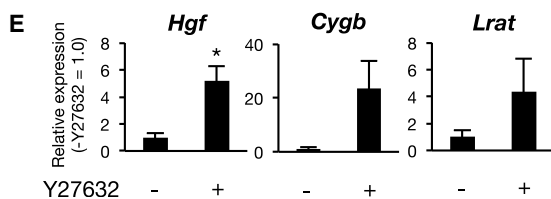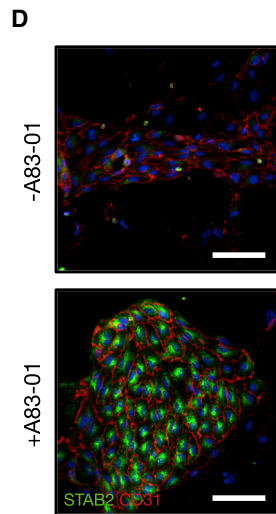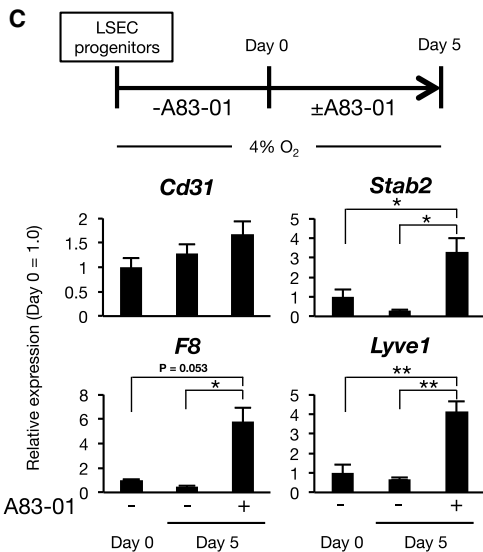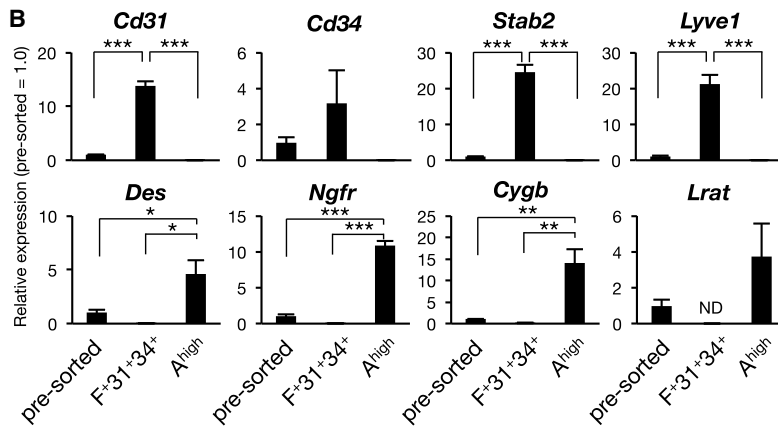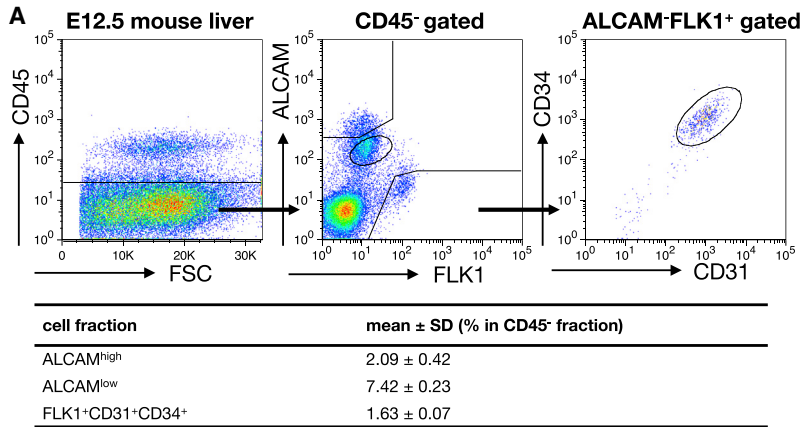
Figure 1. Identification of Fetal Mouse LSEC/HSC Progenitors and Efficient Culture Systems for Each Progenitor

(A) FCM analysis of fetal mouse liver cells at E12.5. CD45$^-$FLK1$^+$ cells, CD45$^-$ALCAM^{high} cells, and CD45$^-$ALCAM^{low} cells were identified (left and middle). CD45$^-$FLK1$^+$ cells also expressed CD31 and CD34 (right). Positive gates were defined by the isotype control. Percentages of each cell population are shown as the mean ± SD of 3 independent experiments (lower panel).

(B) qRT-PCR analysis of LSEC progenitor and HSC progenitor marker genes in pre-sorted cells (pre-sorted), CD45$^-$FLK1$^+$CD31$^+$CD34$^+$ cells (F$^+$31$^+$34$^+$), and CD45$^-$ALCAM^{high} cells (A^{high}). n = 3 in each group (each experiment contains 2 technical replicates). The results are shown as the mean ± SEM. *p < 0.05, **p < 0.01, ***p < 0.001.

(C) (Upper) Schematic representation of the culture system for mouse LSEC progenitors. (Lower) Expression levels of the endothelial marker (Cd31) and LSEC-specific markers (Stab2, F8, and Lyve1) in CD45$^-$FLK1$^+$CD31$^+$CD34$^+$ LSEC progenitors with or without A83-01 treatment (day 5). CD45$^-$Flk1$^+$CD31$^+$CD34$^+$ LSEC progenitors were used as a control (day 0). The results are shown as the mean ± SEM of 3 independent experiments (each experiment contains 2 technical replicates). *p < 0.05, **p < 0.01.

(D) Immunofluorescence staining for LSEC markers in CD45$^-$FLK1$^+$CD31$^+$CD34$^+$ LSEC progenitors after 5 days of culture with or without A83-01 treatment. STAB2 (green) and CD31 (red). Nuclei were counterstained with Hoechst 33342 (blue). Scale bars, 100 μm.

(E) Expression levels of the HSC markers in CD45$^-$ALCAM^{high} HSC progenitor cells with or without Y27632 treatment for 5 days. The results are shown as the mean ± SEM of 3 independent experiments (each experiment contains 2 technical replicates). *p < 0.05.

See also Figure S1.

CD45⁻FLK1⁺ endothelial cells and CD45⁻ALCAM^{high} mesenchymal cells were clearly detected in the fetal livers at E12.5, and we found that CD45⁻FLK1⁺ endothelial cells also expressed CD31 and CD34. Consistently, qRT-PCR analysis showed that CD45⁻FLK1⁺CD31⁺CD34⁺ cells isolated from fetal livers expressed LSEC marker genes such as *Stab2* and *Lyve1* (Figure 1B), suggesting that they are LSEC progenitors. On the other hand, CD45⁻ALCAM^{high} cells expressed HSC marker genes such as *Des*, *Ngfr*, *Cygb*, and *Lrat* (Figure 1B), suggesting that they are HSC progenitors. FCM analysis of fetal liver cells revealed the presence of CD45⁻ALCAM^{low} cells (Figure 1A). As ALCAM has been reported to be weakly expressed in hepatoblasts (Asahina et al., 2009), we examined whether CD45⁻ALCAM^{low} cells expressed hepatoblast markers and revealed that they expressed *Hnf4a*, *Afp*, and *Alb* (Figure S1A), indicating that they are hepatoblasts. These results suggest that a combination of these specific cell-surface markers could be used to enrich for LSEC progenitors and HSC progenitors from differentiating hiPSCs.

Development of Efficient Culture Systems for LSEC Progenitors and HSC Progenitors

To produce large quantities of mature LSECs and HSCs, we sought to establish culture systems that allow the expansion and maturation of CD45⁻FLK1⁺CD31⁺CD34⁺ LSEC progenitors and CD45⁻ALCAM^{high} HSC progenitors, which were isolated from mouse fetal livers. Importantly, CD45⁻FLK1⁺CD31⁺CD34⁺ LSEC progenitors were highly proliferative (Figure S1B), and maintained their characteristics after expansion *in vitro* (data not shown). Because our previous study revealed that transforming growth factor β (TGFβ) signaling inhibits maturation of LSECs from mouse embryonic stem cells (Nonaka et al., 2008), we then evaluated the differentiation potential of expanded CD45⁻FLK1⁺CD31⁺CD34⁺ LSEC progenitors. After induction of LSEC maturation by inhibiting TGFβ signaling using A83-01, a TGFβRI inhibitor, in the hypoxic culture (Figure 1C), mature LSEC-specific markers such as *Stab2*, *F8*, and *Lyve1* were highly upregulated compared with the control (without A83-01) (Figures 1C and 1D). On the other hand, signals for survival and differentiation of HSC progenitors have not been elucidated. Although the Rho signaling pathway was reported to play a role in the activation of mature HSCs (Murata et al., 2001), its effect on HSC progenitors was unknown. We assessed the role of the Rho signaling pathway in CD45⁻ALCAM^{high} HSC progenitors by inhibiting ROCK, an effecter of Rho, and found that they proliferated in the presence of Y27632, a potent ROCK inhibitor (Figure S1C). Moreover, after cultivation in the presence of Y27632, the cells highly expressed mature HSC marker genes such as *Hgf*, *Cygb*, and *Lrat*

(Figure 1E). These results suggested that the Rho signaling pathway regulates the proliferation and maturation of HSC progenitors. Taken together, these data demonstrated that FLK1⁺CD31⁺CD34⁺ LSEC progenitors and ALCAM^{high} HSC progenitors could be expanded *in vitro* while maintaining their potential to become mature cells.

Generation of hiPSC-Derived LSEC Progenitors

To develop an efficient culture system for producing mature LSECs from hiPSCs, we attempted to generate LSEC progenitors capable of proliferating and differentiating into mature LSECs *in vitro*. It is well established that endothelial cells arise from mesodermal cells during embryogenesis. Likewise, LSEC progenitors are considered to have arisen from mesodermal cells. Therefore, we developed a differentiation system for LSEC progenitors after the induction of hiPSCs into mesodermal cells according to the published protocol with some modifications (Kattman et al., 2011; White et al., 2013) (Figure 2A). We assessed the differentiation of hiPSCs by qRT-PCR analysis. The expression of the pluripotency marker gene, *OCT4*, was decreased, whereas the expression of the mesodermal marker, *MESP1*, was increased along with mesodermal differentiation (Figure S2A). The endothelial marker genes, *CD31* and *CDH5* (VE-cadherin), were highly expressed in hiPSC-derived cells at the endothelial progenitor stage (Figure S2A). Surprisingly, the LSEC marker genes *STAB2* and *LYVE1* were also upregulated at this stage (Figure S2A). We therefore tested whether FLK1⁺CD31⁺CD34⁺ LSEC progenitors were generated in the culture. Interestingly, FCM analysis showed that FLK1⁺CD31⁺CD34⁺ and FLK1⁺CD31⁺CD34⁻ cells were already present in the differentiation stage by this culture system (Figure 2B). To further characterize these cells, we isolated CD34⁺ and CD34⁻ fractions and analyzed their gene expression patterns. Sorted FLK1⁺CD31⁺CD34⁺ cells highly expressed LSEC-specific genes such as *STAB2*, *LYVE1*, and *FLT4* compared with pre-sorted cells and FLK1⁺CD31⁺CD34⁻ cells (Figure 2C). On the other hand, the FLK1⁺CD31⁺CD34⁻ cell population highly expressed pluripotent marker and mesenchymal markers compared with the FLK1⁺CD31⁺CD34⁺ cell population (data not shown). These results suggested that FLK1⁺CD31⁺CD34⁺ cells derived from hiPSCs exhibit characteristics of LSEC progenitors in the mouse fetal liver. FLK1⁺CD31⁺CD34⁺ LSEC progenitor cells derived from hiPSCs proliferated and exhibited morphology similar to that of endothelial cells (stage 3) (Figures 2A and S2B). These cells were highly proliferative (Figure S2C) and could be expanded for several passages (Figure S2D). Furthermore, serially cultured cells maintained high expression levels of the LSEC progenitor markers *FLK1*, *CD34*, *CD31*, *CDH5*,
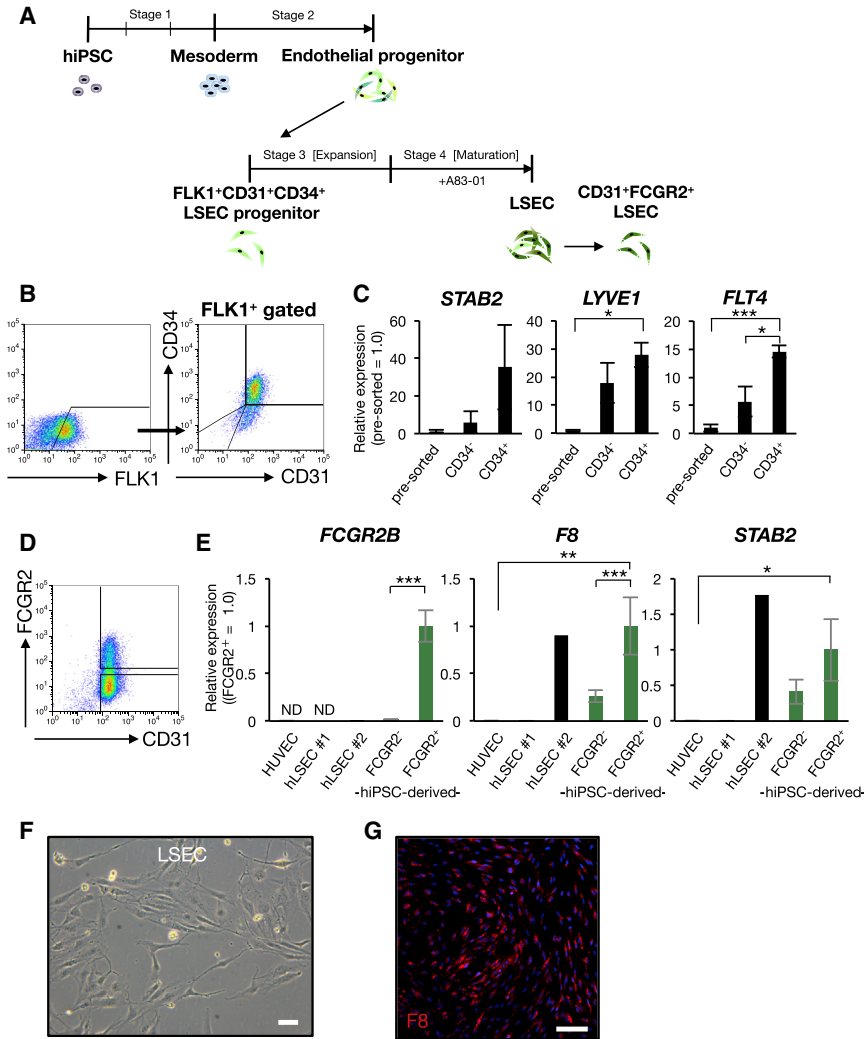
Figure 2. Generation of hiPSC-Derived LSECs

(A) Schematic representation of LSEC differentiation from hiPSCs.

(B) FCM analysis of hiPSC-derived endothelial progenitor stage. FLK1$^+$ cells were identified (left), and CD31$^+$CD34$^{+/-}$ cells were identified in FLK1$^+$ cell fraction (right).

(C) Expression levels of LSEC-specific markers in hiPSCs-derived FLK1$^+$CD31$^+$CD34$^+$ cells (CD34$^+$) compared with FLK1$^+$CD31$^+$ CD34$^-$ cells (CD34$^-$) and pre-sorted cells (pre-sorted). The results are shown as the mean ± SEM of 3 independent experiments (each experiment contains 2 technical replicates). *p < 0.05, ***p < 0.001.

(D) FCM analysis of CD31 and FCGR2 in hiPSCs-derived LSECs.

(E) Expression levels of the mature LSEC-specific marker genes (*FCGR2B*, *STAB2*, and *F8*) in HUVECs (n = 3), primary human LSECs (2 different lots, n = 1, 1), hiPSC-derived CD31$^+$FCGR2$^-$ cells (FCGR2$^-$, n = 10), and CD31$^+$FCGR2$^+$ mature LSECs (FCGR2$^+$, n = 10). The results shown are mean ± SEM of independent experiments (each experiment contains 2 technical replicates). *p < 0.05, **p < 0.01, ***p < 0.001. ND, not detected.

(F) Phase-contrast image of CD31$^+$FCGR2$^+$ mature LSECs. Scale bar, 100 μm.

(G) Immunofluorescence staining for F8 (red) in mature LSECs. Nuclei were counterstained with Hoechst 33342 (blue). Scale bar, 100 μm.

See also Figure S2.

STAB2, and *LYVE1* (Figure S2E). Additionally they could be cryopreserved without phenotypic changes (Figure S2F). Collectively these data indicated that FLK1$^+$CD31$^+$CD34$^+$ cells derived from hiPSCs are LSEC progenitors.

Maturation of LSECs from hiPSC-Derived LSEC Progenitors

As FLK1$^+$CD31$^+$CD34$^+$ LSEC progenitors from fetal mouse livers differentiated into mature LSECs by inhibiting TGFβ signaling in hypoxic culture conditions (Figures 1C and 1D), we investigated whether hiPSC-derived LSEC progenitors undergo functional maturation in our culture system (Figure 2A). After culturing in the presence of A83-01 under hypoxic conditions for 14 days, the expression levels of the mature LSEC markers, *FCGR2B*, *STAB2*, *F8* (Factor VIII), and *LYVE1*, were highly upregulated (Figure S2G). Because FCGR2 was detected only in

mature LSECs from adult mouse livers (Nonaka et al., 2007), we enriched the CD31$^+$FCGR2$^+$ population by using a cell sorter and defined them as hiPSC-derived mature LSECs (Figure 2D). qRT-PCR analysis showed that the LSEC-specific marker genes *FCGR2B*, *STAB2*, and *F8* were highly expressed in CD31$^+$FCGR2$^+$ LSECs compared with CD31$^+$FCGR2$^-$ cells and human umbilical vein endothelial cells (HUVECs) (Figure 2E). In addition, these expression levels were comparable with or much higher than those in primary human LSECs. Isolated CD31$^+$FCGR2$^+$ mature LSECs could also be cultured after several passages and exhibited typical mature endothelial morphology (Figure 2F). Immunohistochemical and FCM analysis showed strong expression of F8, a specific marker of mature LSECs (Figures 2G and S2H). These results demonstrated that inhibition of the TGFβ signaling pathway in hypoxic culture promotes the functional
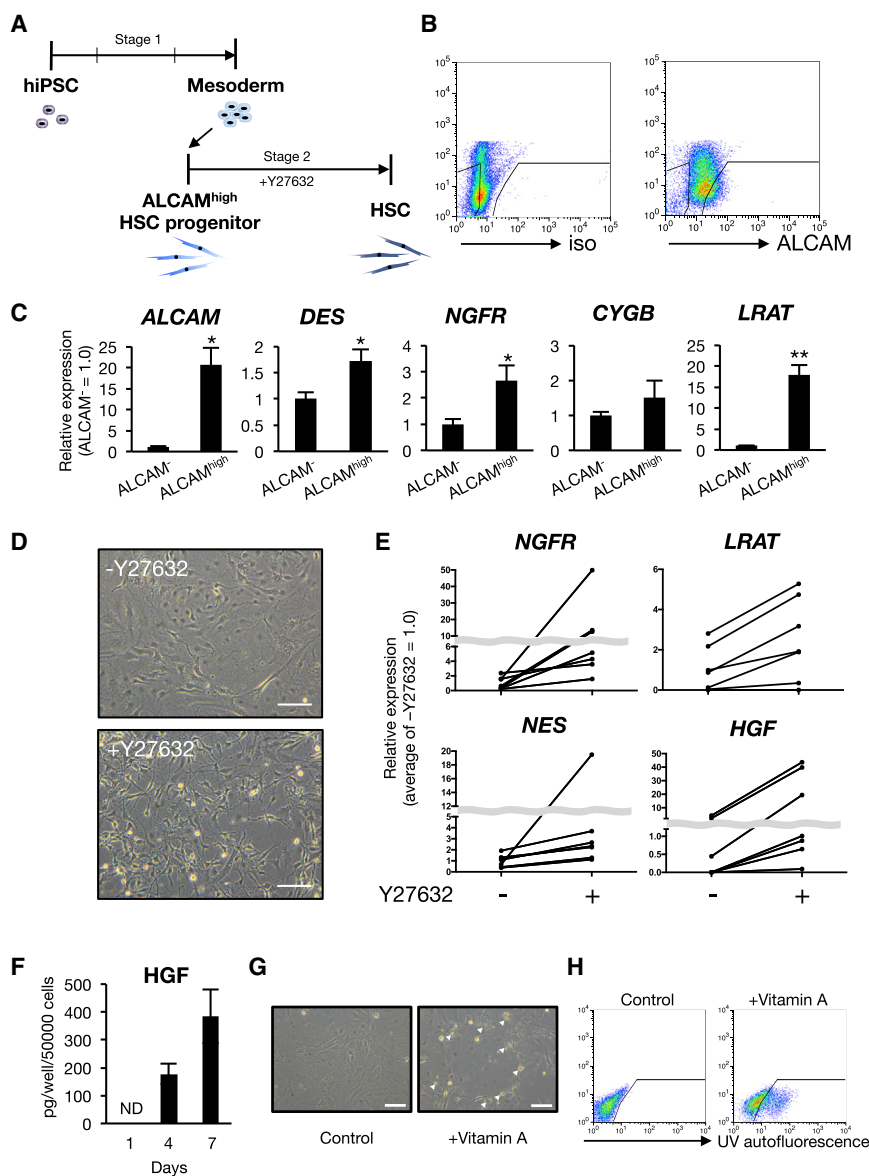
Figure 3. Generation of hiPSC-Derived HSCs

(A) Schematic representation of HSC differentiation from hiPSCs.

(B) FCM analysis of ALCAM in hiPSC-derived mesodermal cells. The positive gate was defined by the isotype control.

(C) Expression levels of HSC markers in hiPSC-derived ALCAM^high HSC progenitors (ALCAM^high) compared with ALCAM^− cells (ALCAM^−). The results are shown as the mean ± SEM of 4 independent experiments (each experiment contains 2 technical replicates). *p < 0.05, **p < 0.01.

(D) Phase-contrast image of hiPSC-derived HSCs with or without Y27632 treatment after 5 days of culture. Scale bars, 100 μm.

(E) Expression levels of the mature HSC marker genes (*NGFR*, *LRAT*, *NES*, and *HGF*) in hiPSC-derived HSCs (iPS-HSC) with or without Y27632 treatment (n = 7). Gene expression was compared between paired samples. Each experiment contains 2 technical replicates.

(F) Secretion levels of HGF during 1 day, 3 days, or 7 days in hiPSC-derived HSCs. The results are shown as the mean ± SEM of 3 independent experiments. ND, not detected.

(G) Phase-contrast image of hiPSC-derived HSCs incubated with retinol (vitamin A). Arrowheads indicate droplets of vitamin A. Scale bars, 100 μm.

(H) FCM analysis autofluorescence of intracellular vitamin A droplets in hiPSC-derived HSCs.

See also Figure S3.

maturation of hiPSC-derived LSECs as well as mouse LSECs.

Generation of hiPSC-Derived HSC Progenitors

To produce a large amount of mature HSCs from hiPSCs, we also aimed to generate HSC progenitors capable of proliferation *in vitro*. We demonstrated that ALCAM is a useful cell-surface marker for the isolation of mouse HSC progenitors (Figures 1A and 1B). Therefore, we evaluated the expression of ALCAM in differentiating hiPSCs by FCM analysis. We developed a two-step protocol to generate mature HSCs from hiPSCs (Figure 3A). As ALCAM^high cells developed after mesoderm differentiation, ALCAM^high and ALCAM^− cells were sorted by using

a cell sorter for further analysis (Figure 3B). ALCAM^high cells strongly expressed HSC marker genes such as *DES*, *NGFR*, *CYGB*, and *LRAT* compared with ALCAM^− cells (Figure 3C). These results suggested that hiPSC-derived ALCAM^high HSC progenitors could be used for the production of mature HSCs.

Maturation of HSCs from hiPSC-Derived ALCAM^high HSC Progenitors

As we had shown that ALCAM^high HSC progenitors isolated from mouse fetal livers were proliferative and differentiated following inhibition of the Rho signaling pathway (Figures 1E and S1C), we sought to compare this result with our hiPSC-derived ALCAM^high HSC progenitors, which were

cultured in the presence of Y27632 (Figure 3A). We found that these cells proliferated (Figure S3A) and exhibited typical mature HSC morphology with projections after 5 days of culture, compared with cells cultured in the absence of Y27632 (Figure 3D). Furthermore, although no significant differences were observed in mRNA expression levels due to variability between experiments, HSC marker genes such as *NGFR*, *LRAT*, and *NES* were markedly increased after treatment with Y27632 (Figure 3E), and the expression levels in hiPSC-derived HSCs treated with Y27632 were much higher than those in human mesenchymal stem cells (MSCs) and primary human HSCs (Figure S3B). Conversely, pluripotency and mesodermal marker genes were reduced to undetectable levels after differentiation (Figure S3C). hiPSC-derived HSCs also expressed high levels of hepatocyte growth factor (HGF) RNA and protein (Figures 3E and 3F), indicating that they may be useful for the generation of functional hepatocytes from hiPSCs. Moreover, because mature HSCs are known to be vitamin A-storing cells, we analyzed this activity in hiPSC-derived HSCs. Vitamin A droplets were observed in hiPSC-derived HSCs (Figure 3G), and FCM analysis of autofluorescence from vitamin A by UV irradiation showed that as much as 35% of hiPSC-derived HSCs stored vitamin A (Figure 3H). However, these vitamin A droplets were not detected in human MSCs (Figures S3D and S3E). As expected, those vitamin A-storing hiPSC-derived HSCs highly expressed HSC marker genes (Figure S3F). These results demonstrated that the Rho signaling pathway plays a critical role in the expansion and differentiation of hiPSC-derived ALCAM^{high} HSC progenitors as well as mouse HSCs.

Expansion and Maintenance of LPCs in a Co-culture System with hiPSC-Derived NPCs

Next, we evaluated the ability of hiPSC-derived NPCs to support the maintenance of LPCs. hiPSC-derived CPM$^+$ LPCs were prepared according to our previous protocol (Kido et al., 2015) and cultured on hiPSC-derived NPC feeder cells for 14 days (Figure 4A). CPM$^+$ LPCs formed many compact colonies on hiPSC-derived NPC feeder cells, whereas very few colonies were formed on collagen I-coated plates (data not shown) and HUVEC/MSC feeder cells, which we used as a control (Figure 4B). Growth rate of CPM$^+$ LPCs on each feeder cell revealed that CPM$^+$ LPCs were highly proliferative on hiPSC-derived NPC feeder cells (Figure 4C). These data indicated that hiPSC-derived NPCs could support proliferation of LPCs. In addition, expression of LPC markers such as *HNF4A*, *AFP*, and *ALB* in CPM$^+$ LPCs was dramatically increased by 14 days of culture on hiPSC-derived NPCs (Figure 4D). In this hiPSC-derived liver co-culture system, AFP was also abundantly detected in the culture medium (Figure S4A). More-

over, we investigated whether the expanded CPM$^+$ LPCs, simply by co-culture with hiPSC-derived NPCs, maintained their potential for differentiation into hepatocytes. After the induction of hepatic maturation by oncostatin M stimulation, hepatocytes from CPM$^+$ LPCs showed typical human hepatocyte morphology (Figure 4E) and were positive for ALB and HNF4A (Figure 4F). In addition, these cells produced a large amount of ALB in the culture medium (Figure S4B). Furthermore, they started to express various metabolic enzyme genes such as *PCK1*, *TAT*, *CPS1*, and *G6PC* (Figure S4C). In sharp contrast, the expression of these liver enzymes was not induced in CPM$^+$ LPCs cultured on HUVECs/MSCs. These data indicated that expanded LPCs maintained their potential for differentiation into hepatocytes. To induce fully functional hepatocytes from hiPSC-derived LPCs, we also established a high-density co-culture system (Figure 4G). hiPSC-derived liver cells expressed some hepatic metabolic enzyme genes at levels comparable with cultured primary human hepatocytes (Figure 4H). We then performed RNA sequencing (RNA-seq) analysis of hiPSC-derived LPCs, hiPSC-derived liver model, and primary human hepatocytes for a more in-depth analysis. Expression of 60 hepatic metabolic enzyme genes was dramatically increased in the hiPSC-derived liver model compared with hiPSC-derived LPCs (Figure 4I). Immature hepatocytes or hepatoblasts marker genes such as *AFP*, *EPCAM*, *CD133*, and *DLK1* were still expressed in the hiPSC-derived liver model (data not shown), indicating that there is still room for improvement on this two-dimensional liver model. Collectively, these results suggest that hiPSC-derived NPCs are able to support proliferation and differentiation of hiPSC-derived LPCs.

Mechanism of hiPSC-Derived NPCs in Supporting Liver Development *In Vitro*

Finally, we performed microarray analysis to understand how hiPSC-derived NPCs regulate LPC maintenance/differentiation. Among the signaling molecules involved in liver development, we identified 31 genes that showed over 2-fold increase in RNA expression in hiPSC-derived LSECs/HSCs compared with HUVECs/MSCs (Figure S4D). These genes include hepatocyte growth and/or differentiation factors such as HGF, fibroblast growth factors, bone morphogenetic proteins, and midkine as well as extracellular matrices (ECMs) such as collagens and laminins. Microarray results were confirmed by qRT-PCR of the three-independent samples (Figure S4E). Although the contribution of NPCs in human liver development is not completely understood, hiPSC-derived NPCs, especially hiPSC-derived HSCs, might have promoted hepatic maturation of hiPSC-derived LPCs in a high-density co-culture system by secreting these hepatic mitogens and ECMs.
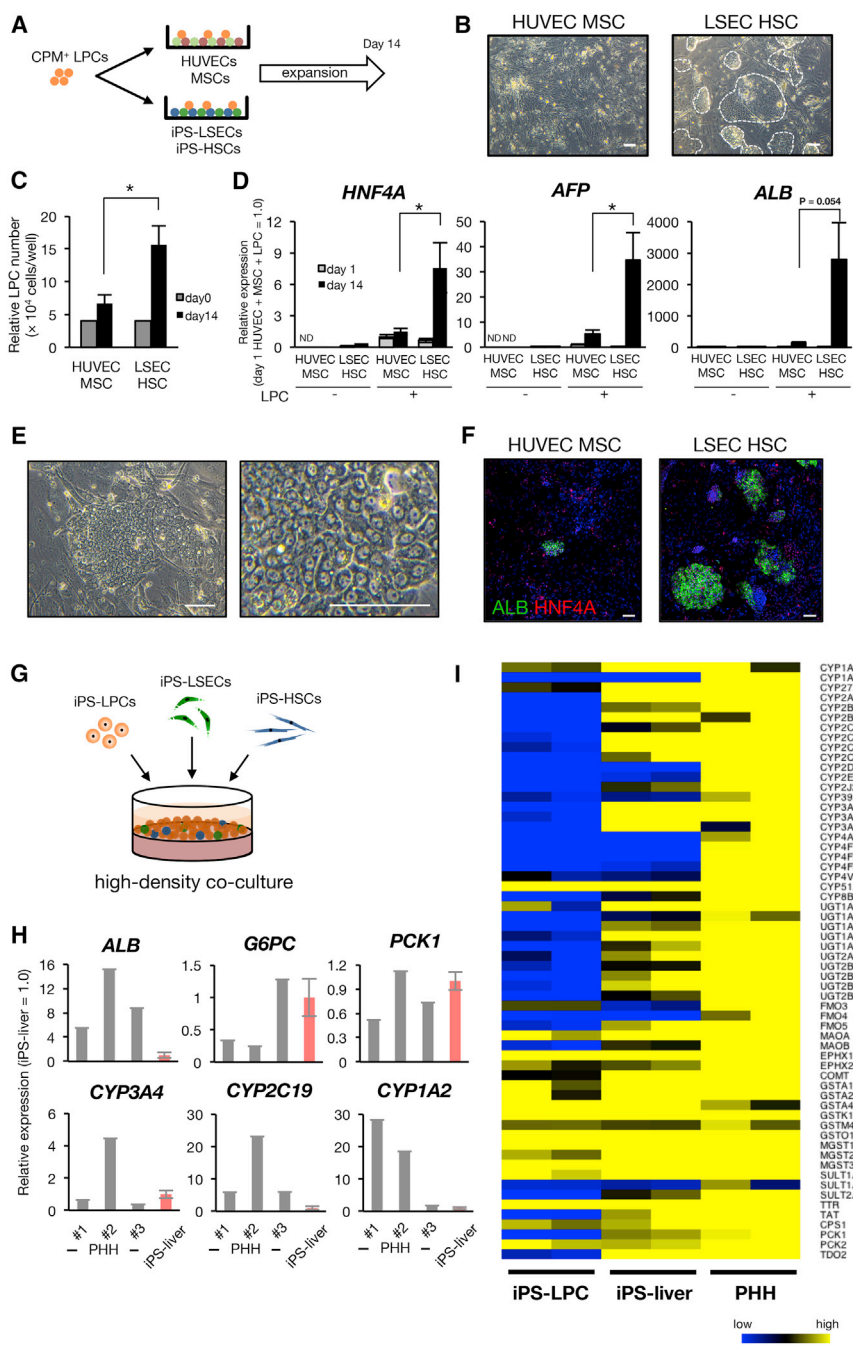
Figure 4. Expansion and Maintenance of LPCs in Co-culture with hiPSC-Derived Liver Cells

(A) Schematic representation of a co-culture system of hiPSC-derived liver cells.

(B) Phase-contrast image of hiPSC-derived CPM$^+$ LPCs on HUVEC/MSC feeder cells (left) or hiPSC-derived NPC feeder cells (right) at day 14. White dashed lines outline colonies of CPM$^+$ hepatoblasts. Scale bars, 100 μm.

(C) Growth rate of CPM$^+$ LPCs in culture for 14 days. The number of feeder cells was subtracted from total cell number in each well. The results are shown as the mean ± SEM of 3 independent experiments. *p < 0.05.

(D) Expression levels of the LPC marker genes at day 1 and day 14 in CPM$^+$ LPCs cultured on HUVEC/MSC feeder cells or hiPSC-derived NPC feeder cells (LSEC/HSC). The results are shown as the mean ± SEM of 9 independent experiments (each experiment contains 2 technical replicates). *p < 0.05. ND, not detected.

(E) Phase-contrast image of hiPSC-derived hepatocytes on hiPSC-derived NPC feeder cells after induction of hepatic maturation. Scale bars, 100 μm.

(F) Immunofluorescence staining for ALB (green) and HNF4A (red) in hiPSC-derived hepatocytes on HUVEC/MSC feeder cells or hiPSC-derived NPC feeder cells after induction of hepatic maturation. Nuclei were counterstained with Hoechst 33342 (blue). Scale bars, 100 μm.

(G) Schematic representation of a high-density co-culture system of hiPSC-derived liver cells.

(H) Expression levels of mature hepatocyte marker genes after induction of terminal hepatic differentiation in hiPSC-derived liver cells (iPS-liver) (n = 3). Human primary cultured hepatocytes were used as control (3 different lots). The results are shown as the mean ± SEM (each experiment contains 2 technical replicates).

(I) Comparison of gene expression levels of hepatic metabolic enzyme genes in hiPSC-derived LPCs (iPS-LPC), hiPSC-derived liver model (iPS-liver), and primary human hepatocytes (PHH) by RNA-seq. Results of RNA-seq are depicted by color (n = 2, 2, 2). See also Figure S4.

Because the interactions between LSECs and HSCs have been considered to contribute to vasculogenesis during liver development *in vivo*, we explored this possibility by microarray and qRT-PCR analysis and showed that hiPSC-derived LSECs and HSCs expressed platelet-derived growth factors (PDGFs)/PDGF receptors and C-X-C chemokine receptor 4 (CXCR4)/CXCL12, which are key molecules for vasculogenesis during liver development (Figures S4F and S4G). Under the three-dimensional co-culture system, hiPSC-derived LSECs formed tube-like structures

(Figure S4H). Thus, hiPSC-derived NPCs play important roles for constituting the LPC niche as well as *in vivo* liver development.

DISCUSSION

Studies on liver development have focused mostly on hepatocytes and biliary cells, whereas molecular details of LSEC/HSC differentiation have remained largely unexplored. In this study, we have identified and isolated LSEC progenitors and HSC progenitors in mouse fetal livers and developed culture systems to expand and differentiate these cells. We found that the TGFβ and Rho signaling pathways, respectively, regulate the proliferation and maturation of LSECs and HSCs. Based on these results, we have developed efficient and reproducible culture systems to generate LSEC and HSC from hiPSC. These hiPSC-derived LSEC progenitors and HSC progenitors could be expanded *in vitro* and exhibited distinct cell-specific characteristics upon induction of maturation. Primary non-parenchyma cells appear to rapidly lose their functions because the expression levels of LSEC- and HSC-specific markers in commercially available primary cells were variable and much lower than hiPSC-derived LSECs and HSCs. Thus, our culture systems provide a means to make LSECs and HSCs with much better functions. Additionally we applied these differentiation systems to two other hiPSC lines. Although the expression levels of various LSEC and HSC marker genes were variable in hiPSC lines, hiPSC-derived cells highly expressed these marker genes compared with HUVECs and human MSCs (Figures S2I and S3G).

Furthermore, these hiPSC-derived NPCs highly expressed several hepatic mitogens and ECMs and supported self-renewal of hiPSC-derived LPCs in the two-dimensional culture system without the need for exogenous cytokines. CPM$^+$ LPCs expanded on hiPSC-derived NPCs can be induced to express various hepatic genes. Takebe et al. (2013) described "organ bud technology" that co-cultures hiPSC-derived endodermal cells with HUVECs and MSCs, which were derived from umbilical cord and bone marrow, respectively. They showed that hiPSC-derived liver buds do not exhibit liver functions but become functional after transplantation in mice. We examined whether HUVECs and MSCs are able to support either proliferation or differentiation of hiPSC-derived CPM$^+$ LPCs and revealed that neither proliferation nor differentiation of LPCs was supported by HUVECs and MSCs, indicating that tissue-specific endothelial cells and mesenchymal cells are necessary for the generation of functional tissue *in vitro*. hiPSC-derived NPCs are ideal cells for generating mature liver tissue *in vitro*, and the hiPSC-derived human liver model will be useful for disease modeling, drug screening, and cell therapy.

EXPERIMENTAL PROCEDURES

Cell Culture

The hiPSC line 454E2 and 409B2 were provided by RIKEN Cell Bank (Okita et al., 2011), and TkDN4-M was provided by the University of Tokyo (Takayama et al., 2010). hiPSCs were maintained on mitomycin C-treated (Wako Pure Chemicals Industries, Osaka, Japan) mouse embryonic fibroblast (MEF) feeder cells. hiPSC-derived NPCs were induced from 454E2, 409B2, and TkDN4-M lines. hiPSC-derived LPCs were prepared from TkDN4-M line according to our previous protocol (Kido et al., 2015).

Co-culture of hiPSC-Derived LPCs and NPCs

To expand hiPSC-derived LPCs, we cultured the cells on mitomycin C-treated (Wako) HUVEC/MSC or hiPSC-derived NPC feeder cells (50,000 cells/cm^2) in DMEM/F12 (Sigma-Aldrich) supplemented with 10% fetal bovine serum (JRH Biosciences), penicillin-streptomycin-glutamine, insulin-transferrin-selenium, N2 supplement, MEM non-essential amino acids solution, L-glutamine (Life Technologies), ascorbic acid (1 mM), nicotinamide (10 mM), N-acetylcysteine (0.2 mM) (Sigma-Aldrich), dexamethasone (1 × 10^{-7} M), Y27632 (5 μM) (Wako), and A83-01 (2.5 μM) (Tocris) for 14 days. To induce hepatic maturation of hiPSC-derived LPCs, we cultured cells in HBM (Lonza) supplemented with HCM SingleQuots (excluding epidermal growth factor) and oncostatin M (20 ng/mL) (PeproTech) for 5 days.

Data Analysis

The F test was performed to evaluate equal variance in the data. Significant differences were determined by Student's two-tailed t test or Welch's two-tailed t test depending on scedasticity. One-way ANOVA followed by Tukey's test was used to determine significant differences between more than two groups.

Further experimental details provided in Supplemental Experimental Procedures.

SUPPLEMENTAL INFORMATION

Supplemental Information includes Supplemental Experimental Procedures, four figures, and two tables and can be found with this article online at http://dx.doi.org/10.1016/j.stemcr.2017.06.010.

AUTHOR CONTRIBUTIONS

Y.K. designed the study, performed experiments, analyzed data, and wrote the manuscript. T.K. and A.M. designed the study, analyzed data, and wrote the manuscript. T.I., H.O., S.-W.C., Y.K., and K.S. performed experiments and analyzed data.

ACKNOWLEDGMENTS

REFERENCES

Asahina, K., Tsai, S.Y., Li, P., Ishii, M., Maxson, R.E., Jr., Sucov, H.M., and Tsukamoto, H. (2009). Mesenchymal origin of hepatic stellate cells, submesothelial cells, and perivascular mesenchymal cells during mouse liver development. Hepatology *49*, 998–1011.

Asahina, K., Zhou, B., Pu, W.T., and Tsukamoto, H. (2011). Septum transversum-derived mesothelium gives rise to hepatic stellate cells and perivascular mesenchymal cells in developing mouse liver. Hepatology *53*, 983–995.

Hentsch, B., Lyons, I., Li, R., Hartley, L., Lints, T.J., Adams, J.M., and Harvey, R.P. (1996). Hlx homeo box gene is essential for an inductive tissue interaction that drives expansion of embryonic liver and gut. Genes Dev. *10*, 70–79.

Kattman, S.J., Witty, A.D., Gagliardi, M., Dubois, N.C., Niapour, M., Hotta, A., Ellis, J., and Keller, G. (2011). Stage-specific optimization of activin/nodal and BMP signaling promotes cardiac differentiation of mouse and human pluripotent stem cell lines. Cell Stem Cell *8*, 228–240.

Kido, T., Koui, Y., Suzuki, K., Kobayashi, A., Miura, Y., Chern, E.Y., Tanaka, M., and Miyajima, A. (2015). CPM is a useful cell surface marker to isolate expandable Bi-Potential liver progenitor cells derived from human iPS cells. Stem Cell Reports *5*, 508–515.

Matsumoto, K., Yoshitomi, H., Rossant, J., and Zaret, K.S. (2001). Liver organogenesis promoted by endothelial cells prior to vascular function. Science *294*, 559–563.

Murata, T., Arii, S., Nakamura, T., Mori, A., Kaido, T., Furuyama, H., Furumoto, K., Nakao, T., Isobe, N., and Imamura, M. (2001). Inhibitory effect of Y-27632, a ROCK inhibitor, on progression of rat liver fibrosis in association with inactivation of hepatic stellate cells. J. Hepatol. *35*, 474–481.

Nonaka, H., Tanaka, M., Suzuki, K., and Miyajima, A. (2007). Development of murine hepatic sinusoidal endothelial cells characterized by the expression of hyaluronan receptors. Dev. Dyn. *236*, 2258–2267.

Nonaka, H., Watabe, T., Saito, S., Miyazono, K., and Miyajima, A. (2008). Development of stabilin2^{+} endothelial cells from mouse embryonic stem cells by inhibition of TGFβ/activin signaling. Biochem. Biophys. Res. Commun. *375*, 256–260.

Ogawa, S., Surapisitchat, J., Virtanen, C., Ogawa, M., Niapour, M., Sugamori, K.S., Wang, S., Tamblyn, L., Guillemette, C., Hoffmann, E., et al. (2013). Three-dimensional culture and cAMP signaling promote the maturation of human pluripotent stem cell-derived hepatocytes. Development *140*, 3285–3296.

Okita, K., Matsumura, Y., Sato, Y., Okada, A., Morizane, A., Okamoto, S., Hong, H., Nakagawa, M., Tanabe, K., Tezuka, K., et al. (2011). A more efficient method to generate integration-free human iPS cells. Nat. Methods *8*, 409–412.

Si-Tayeb, K., Noto, F.K., Nagaoka, M., Li, J., Battle, M.A., Duris, C., North, P.E., Dalton, S., and Duncan, S.A. (2010). Highly efficient generation of human hepatocyte-like cells from induced pluripotent stem cells. Hepatology *51*, 297–305.

Takayama, N., Nishimura, S., Nakamura, S., Shimizu, T., Ohnishi, R., Endo, H., Yamaguchi, T., Otsu, M., Nishimura, K., Nakanishi, M., et al. (2010). Transient activation of c-MYC expression is critical for efficient platelet generation from human induced pluripotent stem cells. J. Exp. Med. *207*, 2817–2830.

Takayama, K., Inamura, M., Kawabata, K., Sugawara, M., Kikuchi, K., Higuchi, M., Nagamoto, Y., Watanabe, H., Tashiro, K., Sakurai, F., et al. (2012). Generation of metabolically functioning hepatocytes from human pluripotent stem cells by FOXA2 and HNF1a transduction. J. Hepatol. *57*, 628–636.

Takebe, T., Sekine, K., Enomura, M., Koike, H., Kimura, M., Ogaeri, T., Zhang, R.R., Ueno, Y., Zheng, Y.W., Koike, N., et al. (2013). Vascularized and functional human liver from an iPSC-derived organ bud transplant. Nature *499*, 481–484.

Tanaka, M., Okabe, M., Suzuki, K., Kamiya, Y., Tsukahara, Y., Saito, S., and Miyajima, A. (2007). Mouse hepatoblasts at distinct developmental stages are characterized by expression of EpCAM and DLK1: drastic change of EpCAM expression during liver development. Mech. Dev. *126*, 665–676.

Tremblay, K.D., and Zaret, K.S. (2005). Distinct populations of endoderm cells converge to generate the embryonic liver bud and ventral foregut tissues. Dev. Biol. *280*, 87–99.

White, M.P., Rufaihah, A.J., Liu, L., Ghebremariam, Y.T., Ivey, K.N., Cooke, J.P., and Srivastava, D. (2013). Limited gene expression variation in human embryonic stem cell and induced pluripotent stem cell-derived endothelial cells. Stem Cells *31*, 92–103.